Journal of Applied Mechanics and Technical Physics, No. 4, 1994

NUMERICAL INVESTIGATION OF DEUTERIUM IMPLOSION IN A CONICAL TARGET

A. A. Charakhch'yan

UDC 537.84

The idea of using conical targets for controlled fusion was published quite a while ago [1]. A conical target can concentrate all the energy from a laser in a small solid angle, while traditional spherically symmetric targets require the laser radiation to be distributed as uniformly as possible over the whole spherical surface. A disadvantage of conical targets is that the cone always deforms during the final compression stage, so the ability to obtain ultradense material is limited. Currently spherical targets produce the highest fusion reaction rate (see [2] for example). Nonetheless experiments with conical targets (see reviews [3, 4]) have produced deuterium plasmas with a fusion reaction rate high enough to be of interest.

Here we model a most unexpected experimental result [5], which still has not been satisfactorily explained. An aluminum flyer at ~ 5.4 km/sec impacted a lead target with a thin aluminum cover; the target was filled with deuterium at ~ 1 atm (Fig. 1). In this experiment the deuterium plasma was heated mostly by the primary shock front; the intensity behind the front was proportional to the square of the flyer velocity. The experimental result [5] — a stable recording of $\sim 10^6$ neutrons per shot — stood out because the flyer velocity was so low. In analogous experiments (gold target, polyethylene flyer, and a neutron yield of $\sim 3 \cdot 10^7$) [6], the flyer velocity was much higher: 40-50 km/sec. Even more impressive is the comparison with a laser compression experiment [7], where the measured particle velocity in the target container was ~ 100 km/sec and the neutron yield was only $(1\text{-}4) \cdot 10^4$.

Unfortunately the experiment [5] was not continued after 1980, and evidently never repeated. At the same time, its authors were convinced the result was reliable and included it in recently published reviews [4, 8].

The material flow described below, like that in a spherical target, has a focal point where the temperature is unbounded at the moment of focus according to the Euler equations.* Accurate computations near such points are complex, even if the temperature is limited by dissipative processes and not by instabilities in the converging shock waves, because a calculation that does not use a self-similar solution requires the grid to become denser near the focal point (see [9] for example). In many calculations, the accuracy problem is ignored near the focal point (see [10] and [11] for example). This approach is valid, because after the primary shock wave passes the focal point and is reflected, the deuterium continues to be heated, first by secondary shock reflections, and then quasi-adiabatically. Therefore inaccuracy in flow calculations, especially for the temperature, near the focal point can hardly have a significant effect on the accuracy of the overall calculation, in particular for the neutron yield. The calculations below also do not pretend to give an accurate plasma temperature in the immediate vicinity of the shock focal point.

The literature contains several examples of calculations of gas compression in conical targets, where the material flow is considered in the target and the compressing piston as well as in the gas. Problems have been examined, in which the focusing at the lateral boundary of the cone has no significant effect on the shape of the inner boundary of the piston [12-14]. The possibility a focusing circumferential aluminum jet could have appeared in the experiment [5] evidently was first shown in [15]. The initial formation stage of such a flow has been modeled numerically with reasonable accuracy [16]. The first two-dimensional numerical modeling [17] of the experiment [5] considered the problem of a hollow cavity. Direct flow through

*The calculation is not unbounded if the detailed wave structure is taken into account. See R. G. Peterson, P. S. Spangler, and G. D. Guthrie, "Shock Focusing Model and Experimental Verification, SBIR Phase II - Shock Focusing Validation," Report BMO-TR-93-36, DET 10, Space and Missile Systems Center, 111 E. Mill Street, San Bernadino, CA 92408-1621 (30 September 1993) — Translator.

Moscow. Translated from Prikladnaya Mekhanika i Technicheskaya Fizika, No. 4, pp. 22-32, July-August 1994. Original article submitted July 13, 1993; revision submitted October 5, 1993.

0021-8944/94/3504-0506$12.50

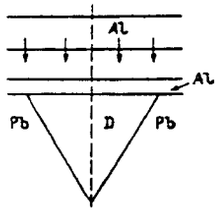

Fig. 1

the material boundaries [18] was used with a grid of $\sim 10^5$ nodes, which were apparently fixed. The initial results of a deuterium-filled cavity [19] were obtained with a first-order method. Explicit lines on the finite-difference grid defined the material boundaries, except for the upper boundary between the aluminum and the lead, which had no significant effect on the deuterium compression dynamics. This approach is much more accurate than using direct flow through the material boundaries. When parameter values close to the experimental ones were used, a circumferential jet of aluminum focusing on the axis of symmetry separated the deuterium into two parts and created a high-velocity jet in it.

Use of a first-order method [19] made it impossible to hope for a correct numerical flow description in grids with 1000–2000 nodes. The use of monotonic high-order methods [20] in the deuterium and aluminum in combination with explicit material boundaries makes it possible to hope for a correct quantitative flow description. Control calculations were done on various grids within the limits of the computer capability.

Here we not only examine the formation and propagation of the high-velocity deuterium jets as was done in [20]; we continue until the jet is completely attenuated and a shock wave forms in the deuterium. The flow is described by Euler's equations. The equation of state for a completely ionized perfect gas is used for deuterium, and a wide-range equation of state [21] is used for the metals. The initial flyer velocity is 5.4 km/sec, the initial deuterium pressure is 1 atm, the flyer thickness is 2 mm, the thickness of the target cover is 0.3 mm, the radius of the hole in the target surface is 1 mm, and the cone angle is 60°.

We do not pretend that our results explain the experiment [5]. Also, the calculated number of neutrons is almost zero, based on the standard formula for the D–D reaction rate as a function of temperature and density [22]. Nonetheless it is clear that the experiment [5] cannot be explained theoretically without understanding the details of shock propagation.

The instability of the aluminum–deuterium boundary can have a large effect on the flow formation (see [23] and [24] for example). This problem is not examined here. Solving it requires calculations with an initially perturbed boundary, along with a purely theoretical analysis. This calculation should be done in the future with a more powerful computer and should include two-dimensional perturbations.

In the figures t is time, and z and r are the axial and radial coordinates. The base of the cone is at $z = 0$ at time $t = 0$.

Flow Description. Figure 2 shows part of the velocity field during the initial compression stage. The solid lines are the material boundaries. An imploding circumferential aluminum jet has already formed. The structure of the shock waves in the deuterium can be seen. One shock wave, from the acceleration of the aluminum inner boundary, has a plane front parallel to the initial position of the aluminum boundary. Two other shock waves come from the imploding jet of aluminum. One moves through the unperturbed deuterium along the base of the cone, while the other moves along the axis of symmetry through the deuterium compressed by the shock wave. This last wave eventually will focus and reflect from the axis of symmetry. Qualitatively the shock waves behave the same as if a shock wave struck the base of a conical target (see [25]).

Figure 3 shows a fragment of the finite-difference grid (the thicker lines are the material boundaries) and the velocity field near the deuterium region immediately before the aluminum converges on the axis of symmetry. The deuterium divides into two parts which hereafter will be called the upper and lower parts. It can be seen that high-velocity jets arise along the axis of symmetry in both parts.

We shall assume that the solution of the Euler equations describes the focusing as follows. Initially the aluminum–deuterium boundary is tangent to the axis of symmetry at one point. Then the point transforms into an expanding segment with ends at the points where the material boundary intersects the axis. The intersection angle α (which is different for each end of the segment) differs from zero at all times except possibly for a short time after the moment of tangency. Then the velocity u_e of the end of the segment is an obvious geometric function of the angle α and the velocity component u_n normal to the material boundary:

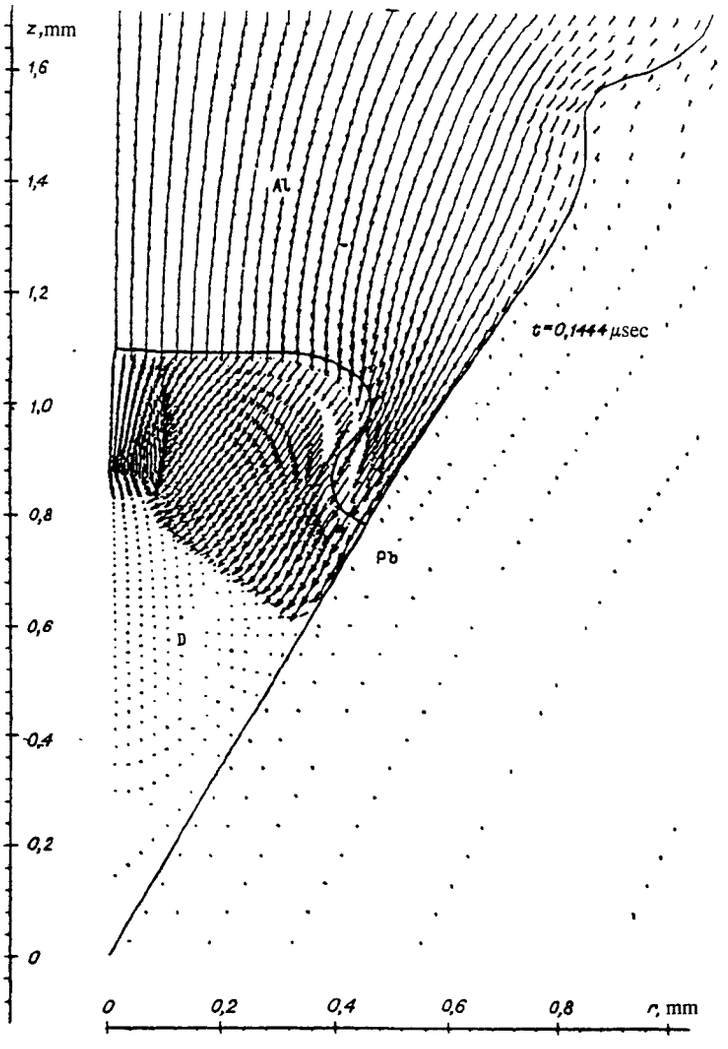

Fig. 2

$$u_e = u_n / \sin\alpha. \tag{1}$$

This behavior of the Euler solution is modeled numerically as follows: As soon as any node of the aluminum–deuterium boundary gets close enough to the axis of symmetry it is moved to the axis and thereafter can move only along it. If the neighboring node is already on the axis, the corresponding series of deuterium cells are discarded, and a symmetry condition is imposed on the boundary of the aluminum cell. Nodes are distributed uniformly along the boundary, until a specified number converge on the axis of symmetry. Afterwards the velocity of the boundary nodes along the axis is calculated from Eq. (1) and the uniform node spacing becomes different for the aluminum strip and for the two parts of the deuterium. As a result the angle α increases and the boundary nodes leave the axis of symmetry. The time step for the explicit method was effectively increased by using this method several times in cells where the specified time step exceeded the time step for stability for that cell.

Dynamics of the aluminum convergence and the formation and propagation of the deuterium jets are shown in Fig. 4. The pressure and velocity distributions along the axis are shown for four sequential times. The lower part shows the corresponding profiles of the deuterium boundary. The dashed line is the axis, and the arrow shows the positive direction along the axis. Just before convergence, the pressure in the narrowest part of the throat is $\approx 30 \cdot 10^6$ atm (Fig. 4a). Then the deuterium pressure drops, a jet breaks away from the aluminum, and, along with the shock waves it generates, moves through the relatively unperturbed deuterium. The maximum deuterium velocity is ≈ 200 km/sec in the upper part and ≈ 180 km/sec in the lower part (Fig. 4b). The jet in the upper part hits the aluminum and moves in the opposite direction (Fig. 4c). The

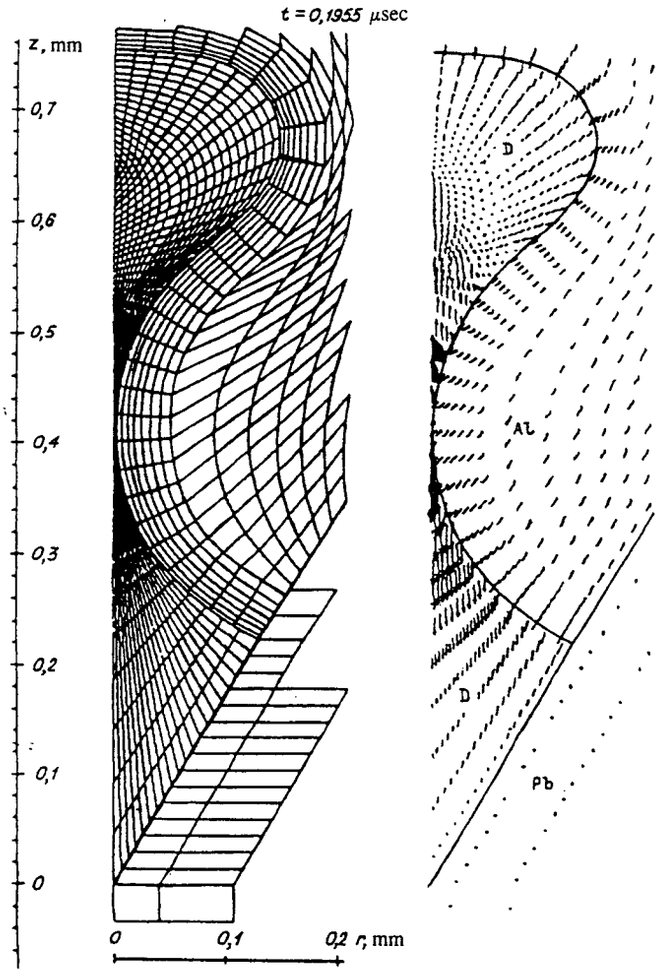
t = 0,1955 μsec
z, mm
0,7
0,6
0,5
0,4
0,3
0,2
0,1
0
D
Al
D
Pb
0
0,1
0,2 r, mm

Fig. 3.

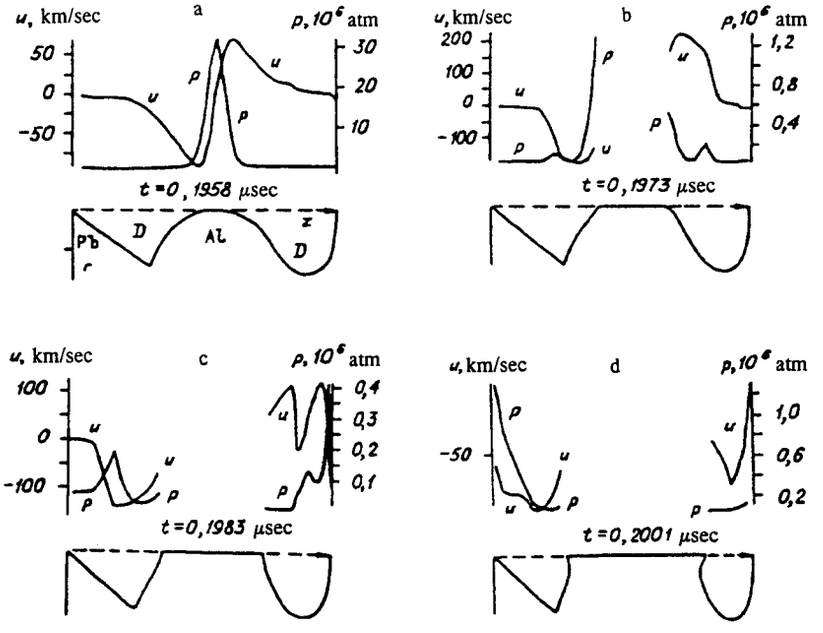
u, km/sec
a
p, 10⁶ atm
50
0
-50
30
20
10
t = 0, 1958 μsec
Pb
D
Al
D
z
r
u, km/sec
b
p, 10⁶ atm
200
100
0
-100
1,2
0,8
0,4
t = 0, 1973 μsec
u, km/sec
c
p, 10⁶ atm
100
0
-100
0,4
0,3
0,2
0,1
t = 0, 1983 μsec
u, km/sec
d
p, 10⁶ atm
-50
1,0
0,6
0,2
t = 0, 2001 μsec

Fig. 4

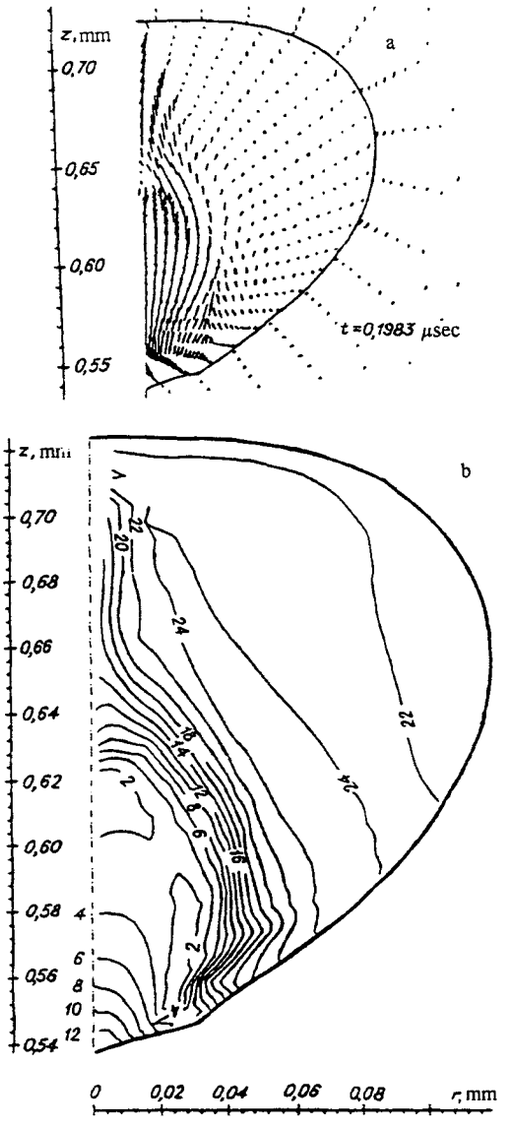

Fig. 5.

other part hits the base of the cone and greatly increases the pressure there (Fig. 4d). This increases the Pb deformation rate, which then limits the pressure growth.

The positive velocity in the upper part of the deuterium in Figs. 4c and 4d reflects the appearance of a reverse jet, whose formation is illustrated in Figs. 5 and 6. Figure 5 shows the velocity and density fields in the upper part of the deuterium after the initial jet has broken away from the aluminum (a is the velocity and b are the isochores $10\cdot[\lg\{\rho,g/cm^3\} + 4]$). It can be seen that a zone of relatively rarefied deuterium forms behind the front of the jet. The surrounding deuterium encroaches into this zone and generates a reverse jet, as shown in Fig. 6, which also shows the temperature field (a is the velocity field and b are the isotherms [eV] in deuterium). The maximum temperature, which is also the maximum for all previous times, is near 60 eV. The main mass of the deuterium is heated much less.

Later, both deuterium masses are compressed by secondary imploding jets of aluminum (Fig. 7).

Figures 8a and 8b show the velocity and pressure (10^5 atm) fields in the upper part of the deuterium just before the secondary imploding jet meets the main mass of aluminum, which is moving in the opposite direction. The maximum deuterium temperature is ≈ 30 eV. The deuterium pressure has almost equilibrated and differs little from the pressure in the surrounding aluminum. Therefore further significant compression and heating in the deuterium is not likely. On the other hand, continuing the calculation would require a different structure in the finite-difference grid in the upper part of the

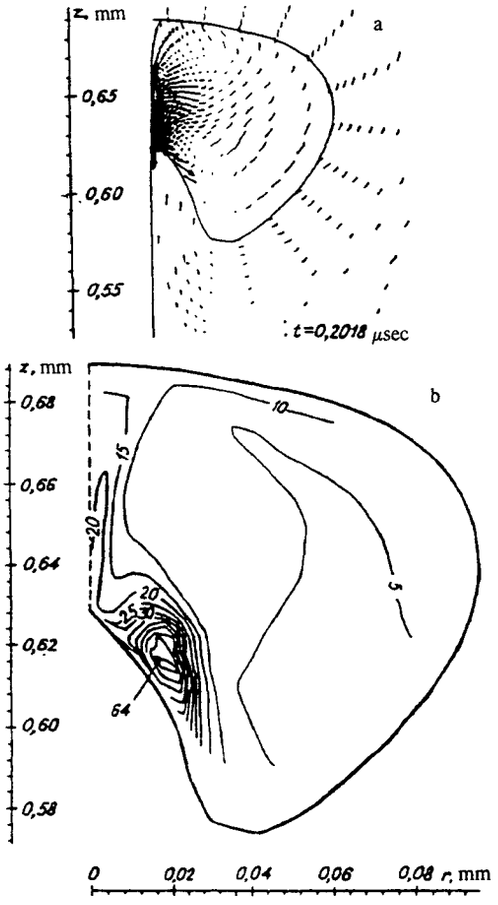

Fig. 6

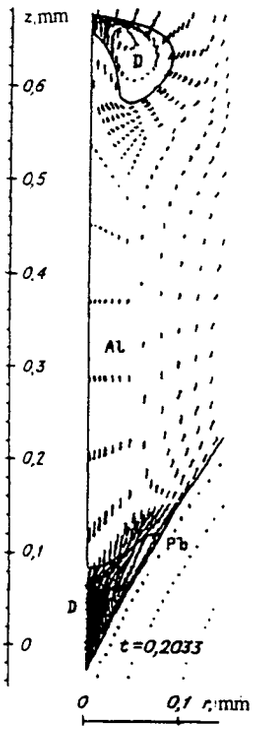

Fig. 7.

deuterium, which would greatly complicate the computer program. For these two reasons the calculation of the upper part of the deuterium was terminated.

The calculation of the lower part of the deuterium was continued until its volume started to expand. The corresponding temperature field is shown in Fig. 9. The maximum temperature ≈ 40 eV and the average temperature ≈ 30 eV both decrease with time. The average density is ≈ 0.2 g/cm^3.

Neutron Yield. After the jets and the resultant shock waves are attenuated, the deuterium temperature is very low (30–40 eV)and differs little from the first-order calculation (≈ 20 eV [19]). The maximum temperature caused by the jet is also small (60–70eV). One-dimensional spherical calculations in [5] were limited by several conditions related to the deformation rate of the lead. The temperatures presented (300–500eV) clearly correspond to the initial velocity of the flyer, which is much greater than 5.4 km/sec; the appearance of these temperatures in [5] is some sort of misunderstanding. At the same time, as noted previously, the authors of the experiment [5] are convinced of the result ($\sim 10^6$ neutrons per shot for a flyer velocity of ~ 5.4 km/sec) and included it in their reviews [4, 8].

The number of neutrons produced were calculated from the standard formula (see [22] for example)

$$N = \int\int w_{DD}(T) n^2/4 dv dt, \qquad (2)$$

$$w_{DD}(T) = 2.6 \cdot 10^{-14} T^{-2/3} \exp(-18.76/T^{1/3}) \text{ cm}^3 \cdot \text{sec}^{-1}$$

where $w_{DD}(T)$ is the D–D reaction rate; T is the temperature, keV; and n is the number of deuterium atoms per unit volume. The integration is carried out over the whole deuterium volume and over time. The number of neutrons N $\approx$ 0, due to the relatively low temperatures.

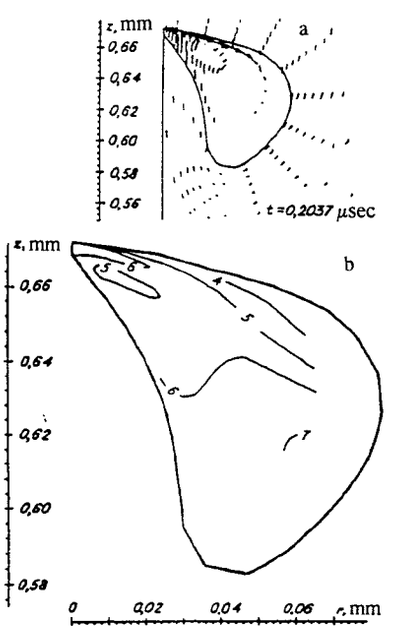

Fig. 8

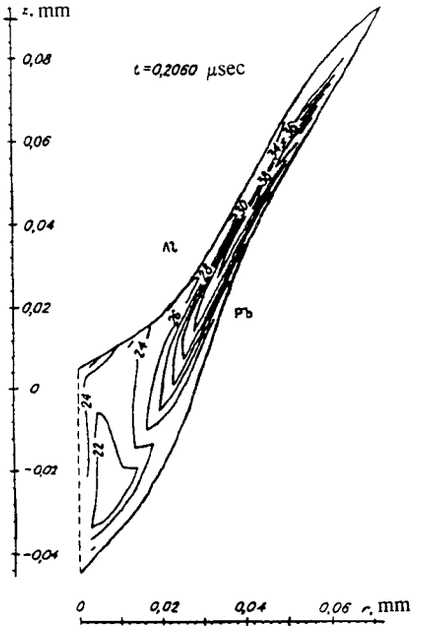

Fig. 9.

We now give a rough lower estimate of the plasma temperature in the experiment [5]. To do this we replace Eq. (2) by an approximation:

$$N = M\tau\bar{\rho}w_{DD}(\bar{T})/4m_D^2. \tag{3}$$

Here M is the mass of the deuterium; τ is the lifetime of the high-temperature plasma; $\bar{\rho}$ and $\bar{T}$ are the characteristic density and temperature of the plasma; and m_D is the nuclear weight of deuterium. Keeping in mind that the deuterium compression calculation was terminated after ~ 0.2 μsec, we set $\tau = 0.1$ μsec. We use $\bar{\rho} = 1$ g/cm^3, which is roughly five times larger than in the calculation. The initial deuterium pressure was ~ 1 atm in the experiment, which gives an initial deuterium density of $\sim 2\cdot 10^{-4}$ g/cm^3. The experimental target parameters (see [4]) — a 53° cone angle and a 1 mm target surface orifice — give $M \approx 4.2\cdot 10^{-7}$ g. With this result and $N = 10^6$ in Eq. (3), we obtain $\bar{T} \approx 0.2$ keV. If the plasma is heated nonuniformly, its maximum temperature should be even higher. This clear disagreement with the above temperature indicates that an effective heating mechanism operates in the plasma that is not included in the Euler equations and therefore is not related solely to plasma compression. At the same time, that an intensive D–D reaction occurred in the experiment in the absence of a high-temperature plasma cannot be excluded. The deuterium jet moving with a velocity of $\sim$180–200 km/sec into relatively quiescent deuterium is analogous to a bundle of heavy water clusters bombarding a deuterated target with a velocity of $\sim$100 km/sec in a published experiment [26], which produced an anomalously large number of protons from the D–D reaction. (There are two D–D reactions which have roughly equal probability: one generates neutrons and the other generates protons [22].) It has been shown [27] that the reaction rate in the experiment [24] cannot depend only on the plasma thermodynamics, because no protons were produced when hydrogen replaced deuterium in either the clusters or the target.

In conclusion we now briefly examine calculated results [20] which go beyond the Euler equations. Two-dimensional Navier–Stokes equations were used to follow how a deuterium plasma in a boundary layer with the aluminum was heated by a high-velocity jet. In this calculation also, the temperature distribution of ions in the boundary layer could not explain the experimental neutron yield. At the same time the solution of the Navier–Stokes equations leaves open the question of local zones with a very high ion temperature, because answering this question requires a viscous heating calculation along the whole jet boundary, not only where it coincides with the boundary of the deuterium. Doing such a numerical investigation is now impossible without a powerful enough computer or a satisfactory adaptive zoning procedure.

How a spontaneous electromagnetic field caused by a high-velocity jet of deuterium plasma affects the flow was investigated numerically using two-dimensional magnetohydrodynamic equations. It was shown that the electromagnetic field did not affect the flow significantly. At the same time, the absolute value of the magnetic field ($\sim 10^4$ G) in the deuterium

can be sufficient to induce experimentally observable currents in the target. If so, then a correlation of the appearance of the currents with the neutron yield would be convincing proof that the yield was related with the implosion of the aluminum. We note that such currents can be measured when laser radiation interacts with matter [28], while the corresponding calculation [29] gives a maximum magnetic field of only 25 G.

The overall conclusion from the results here and in [20] is as follows. The author's multi-year effort to explain the experiment [5] is currently unsuccessful: the experimental neutron yield should have been negligible for the calculated deuterium plasma temperature.

The author thanks Yu. D. Shmyglevskiĭ for a discussion of the results.

REFERENCES

1. F. Winterberg, "Implosion of a dense plasma by hypervelocity impact," Plasma Phys., **10**, No. 1 (1968).
2. S. Nakai, K. Mima, Kh. Azechi, et al., "Prospects of igniting a thermonuclear reaction in the GEKKO XII facility according to the LTS program," Kvantovaya Élektron., **19**, No. 10 (1992).
3. I. V. Sokolov, "Hydrodynamic focusing processes in plasma physics," Usp. Fiz. Nauk, **160**, No. 11 (1990).
4. V. I. Vovchenko, I. K. Krasyuk, P. P. Pashinin, et al., "Pulse compression and heat of a gas in conical targets," Transactions of the Institute of General Physics of the Academy of Sciences (IOFAN) [in Russian], Nauka, Moscow (1992), Vol. 36.
5. S. I. Anisimov, V. E. Bespalov, V. I. Vovchenko, et al., "Neutron generation during the explosive initiation of the D–D reaction in conical targets," Pis'ma Zh. Éksp. Tekh. Fiz., **31**, No. 1 (1980).
6. G. Derentovich, "Strong compression of matter using the focused energy of an explosive," Prikl. Mekh. Tekh. Fiz., No. 1 (1989).
7. V. I. Vovchenko, T. B. Volyak, Yu. S. Kas'yanov, et al., "Characteristics of the interaction of laser radiation with encased targets," Preprint No. 179 [in Russian], Institute of General Physics of the Academy of Sciences (IOFAN), Moscow (1987).
8. A. V. Bushman, I. K. Krasyuk, B. P. Kryukov, et al., "Numerically modeling gas dynamic phenomena in conical targets," Preprint No. 6-278 [in Russian], Institute of High Temperatures of the Academy of Sciences (IVTAN), Moscow (1989).
9. A. I. Marchenko and V. V. Urban, "Calculating focusing shock waves," Prikl. Mekh. Tekh. Fiz., No. 2 (1988).
10. Yu. V. Afanas'ev, P. P. Volosevich, E. G. Gamaliĭ, et al., "Laser compression of glass targets," Pis'ma Zh. Éksp. Tekh. Fiz., **23**, No. 8 (1976).
11. V. A. Gal'burg and M. F. Ivanov, "Dynamics of gas compression by spherical shells considering ionization," Preprint No. 2-079 [in Russian], Institute of High Temperatures of the Academy of Sciences (IVTAN), Moscow (1981).
12. R. J. Mason, R. J. Fries, and E. H. Farnum, "Conical targets for implosion studies with a CO_2 laser," Appl. Phys. Lett., **34**, No. 1 (1979).
13. M. D. Taran, V. F. Tishkin, A. P. Favorskiĭ, et al., "Modeling the implosion of quasi-spherical targets in solid-state cones," Preprint No. 127 [in Russian], Institute of Applied Mathematics of the Academy of Sciences, Moscow (1980).
14. V. V. Demchenko and A. S. Kholodov, "Numerical investigation of the compression and heating of conical targets," Prikl. Mekh. Tekh. Fiz., No. 6 (1985).
15. V. Ya. Ternovoĭ, "Jet formation during plasma compression in acute-angled geometry," Prikl. Mekh. Tekh. Fiz., No. 5 (1984).
16. V. V. Rasskazova, V. G. Rogachev, and N. F. Svidinskaya, "Two-dimensional gas dynamic effects when a shell moves in a conical solid-angled target," VANT Series on the Methods and Programs for Numerical Solution of Problems of Mathematical Physics [in Russian] (1985), No. 3.
17. A. V. Bushman, I. K. Krasyuk, B. P. Kryukov, et al., "Focusing effects during pulsed excitation in conical targets," Pis'ma Zh. Tekh. Fiz., **14**, No. 19 (1988).
18. V. A. Agureĭkin and B. P. Kryukov, "Individual particle method for calculating the flows of multicomponent media with large deformations," ChMMSS, **17**, No. 1 (1986).
19. A. A. Charakhch'yan, Numerical Modeling of Gas Compression in Conical Solid-State Targets [in Russian], Computation Center of the Academy of Sciences, Moscow (1988).

20. A. A. Charakhch'yan, "Calculation of deuterium compression in a conical target within the framework of the Navier–Stokes equations for two-dimensional magnetohydrodynamics," Zh. Vys. Mat. Mat. Fiz., **33**, No. 5 (1993).
21. A. V. Bushman, G. I. Kanel', A. L. Ni, and V. E. Fortov, Thermophysics and Dynamics of Intense Pulsed Loads [in Russian], Institute of Chemical Physics of the Academy of Sciences, Chernogolovka (1988).
22. Keith Bruckner and S. Jorna, Controlled Laser Fusion [Russian translation], Atomizdat, Moscow (1977).
23. R. D. Richtmeyer, "Taylor instability in shock acceleration of compressible fluids," Communications Pure and Appl. Math., **13**, No. 2 (1960).
24. E. E. Meshkov, "Some results of experimental research on the gravitational instability of boundaries separating materials of different density," Investigation of the Hydrodynamic Instability using Computers [in Russian], Institute of Applied Mathematics of the Academy of Sciences, Moscow (1981), pp. 163–190.
25. R. E. Setchell, E. Storm, and B. Sturtevant, "An investigation of shock strengthening in a conical convergent channel," J. Fluid Mech., **56**, No. 3 (1972).
26. R. F. Beuler, G. Friedlander, and L. Friedman, "Cluster-impact fusion," Phys. Rev. Lett., **63**, No. 12 (1989).
27. V. B. Leonas, "New approach to carrying out the D–D fusion reaction," Usp. Fiz. Nauk, **160**, No. 11 (1990).
28. É. M. Barkhudarov, G. V. Gelashvili, G. G. Gumbaridze, and M. I. Taktakishvili, "Efficiency of transforming laser radiation into electrical energy," Kvantovaya Élektron., **14**, No. 9 (1987).
29. N. S. Zakharov, I. S. Shaínoga, and N. I. Shentsev, "Generating magnetic fields in solid targets with coupled pulsed radiation," Kvantovaya Élektron., **16**, No. 2 (1989)